

Evaluation of WEDM performance characteristics and prediction of machining speed during taper square profiling on Hastelloy-X

I.V. Manoj & S Narendranath

To cite this article: I.V. Manoj & S Narendranath (2021): Evaluation of WEDM performance characteristics and prediction of machining speed during taper square profiling on Hastelloy-X, Australian Journal of Mechanical Engineering, DOI: [10.1080/14484846.2021.1960670](https://doi.org/10.1080/14484846.2021.1960670)

To link to this article: <https://doi.org/10.1080/14484846.2021.1960670>



Published online: 08 Aug 2021.



Submit your article to this journal 



View related articles 



View Crossmark data 



ARTICLE



Evaluation of WEDM performance characteristics and prediction of machining speed during taper square profiling on Hastelloy-X

I.V. Manoj and S Narendranath

Department of Mechanical Engineering, National Institute of Technology Karnataka, Surathkal <i>India</i>

ABSTRACT

Hastelloy-X is one of the wrought nickel-base superalloy comprising of oxidation resistance and high-temperature strength. Wire electric discharge machining process is the favoured technique for precise component fabrication of such materials. Apart from precision the most essential aspect with surface integrity and cutting velocity in manufacturing. This investigation deals with the effects of cutting speed override, corner dwell time, wire guide distance and wire offset on taper profile response characteristics. The variation of these parameters is studied by machining a simple square profile at 0°, 15° and 30° taper angles. It is observed that as the taper angle gets increased, both the machined errors at corners and machined roughness increased although the machining speed gets reduced. The recast layer and micro-hardness are explored for the taper square profile components. It is observed that the recast layer thickness was least for 30° taper profiles indicating least thermal degradation which was validated by micro-hardness. It was established that in a machined profile, that corners possessed lower hardness than the edges. The micro-hardness of inner profile corners was found to be lower than outer profile corners. Adaptive neuro-fuzzy interference system is better prediction computing method having least error ranging from 0–4.89%. In conclusion, the machining speed and taper angle also contribute to the output characteristics in wire electric discharge taper profiling.

ARTICLE HISTORY

Received 11 February 2021

Accepted 22 July 2021

KEYWORDS

Taper square profile; machining speed; machining roughness; machining errors; artificial neural network; Adaptive Neuro-Fuzzy Interference System

1. Introduction

Nickel-based alloys have high-temperature strength, creep resistance, oxidation resistance, and corrosion resistance. This enables it to be used in a variety of applications in different industries like petrochemical, nuclear, aerospace, marine, etc. Machining such superalloy materials like nickel-based, cobalt-based, iron/nickel-based, and titanium-based alloys, ceramics are challenging due to high-temperature strength and low thermal conductivity (Naresh Chakala, Chandrabose, and Rao 2019; Raj, S. and Prabhu 2017; Somvir, Dixit, and Kumar 2018). Wire electric discharge machining (WEDM) provides a beneficial solution in machining for such alloys with complex shapes having precision [4]. Abyar et al (Abyar, Abdullah, and Shafaroud 2019) have experimentally and theoretically analyzed the machining errors of the arced paths through successive machining stages. It was also found that the accuracy improved by 83–78% by the compensation calculated from the mathematical model. Abyar et al. (Abyar, Abdullah, and Akbarzadeh 2018) performed profiling of small arced corners through WEDM, where they reported that wire deflection contributed over 57% of total machining errors. The wire vibration and excitation of discharges during machining were the main reasons for the occurrence of machining errors. Bisaria and

Shandilya (Bisaria and Shandilya 2019) have stated that the angle profile corner radius was affected by wire deflection and wire vibration. It was concluded that the corner error was decreased by 29.04%–43.38% for different angles of profile corners at low pulse parameters. Naveed et al. (Naveed et al. 2019) investigated a machining complex taper profile through WEDM. The optimised process gave 33.3% and 14.3% reduction in angular error and radial error of profile. Whereas cutting speed and surface finish improved by 12% and 14.4% during machining. Werner (Werner 2016) reported accurate machining of curvilinear profile by modifying the nominal geometric models of the machined objects. This modification was based on pre-determined deviations obtained through the previous machining. Chen et al. (Chen et al. 2018) have proposed a unique method of cut-back and surface microstructures wire electrode to reduce corner error. There was 87% reduction in corner error by this method during rough corner-cutting.

Shayan et al (Vazini and Afza 2013) have employed back propagation neural network (BPNN) for forecasting the cutting velocity, oversized (overcut) and surface roughness. It was concluded that BPNN generates accurate prediction rather than mathematical modelling. Nayak et al. (Nayak and Mahapatra 2016) performed tapering by WEDM on cryo-treated

Inconel 716 where the artificial neural network was used as a model to determine the relationship between input parameters and performance characteristics. Backpropagation neural network in combination with Levenberg–Marquardt algorithm was employed in modelling as the training of artificial neural network (ANN) becomes faster. Naresh et al (Naresh, Bose, and Rao 2020) have used adaptive Neuro-Fuzzy Interference System (ANFIS) and artificial neural network (ANN) for the prediction of surface roughness and material removal rate. It was concluded that ANFIS with gaussian type membership function gave accurate prediction results than any other results. Suganthi et al (Suganthi et al. 2013) formulated models of ANFIS and backpropagation-based ANN models for the prediction of responses like material removal rate, surface roughness and tool wear ratio in micro EDM. ANFIS model gave the least average absolute percentage errors being 4.33%, 7.49%, and 6.37% for respective parameters.

From the literature, it can be observed that the various input parameters have a different effect on profiling response parameters. The tapering angles were considered from 0° to 30° because of the applications and workpiece thickness for the analysis of response parameters. In this study, an innovative method that avoids the obstacles like wire breakage, guide wear, angular inaccuracies, improper flushing, etc., during tapering in WEDM have been employed. A unique slant type taper fixture is used for obtaining taper profiles for 0°, 15° and 30°. These taper square profiles were machined using L₁₆ orthogonal array for each taper angle. the variation and influence of unexplored profiling parameters like cutting speed override (CSO), corner dwell time (CDT), wire guide distance (WDG) and wire offset (WO) on different response parameters were studied. The machining speed (MS), machining roughness (MR), taper machined errors, recast layer thickness and hardness variation at WEDMed taper corners and surface (edges) were explored for a taper square profile. ANN and ANFIS modelling are used for the prediction of machining speeds for various parameters at different taper angles.

2. Workpiece material and process

2.1. Workpiece material

Hastelloy X is named after ‘Haynes Stellite Alloy’ a nickel-based alloy. It has high mechanical properties and high-temperature strength. Hastelloy X is used in

various high-temperature applications like tailpipes, flame holders, combustor cans, spray bars, afterburners, etc. Composition of the as-received alloy is shown as in Table 1 which was tested from (Optical emission spectrometry) ‘SpectraMax 130,779’ at Quality Test Laboratory, Mumbai, India. The as-received plate is cut to 260 mm×22 mm×10 mm for machining the slot. The alloy was solution heat-treated at 2150°F (1177°C) and rapid cooled which was followed as established from the literature (Chandler 2006).

2.2. Experimental particulars

A square profile of sides 1 mm, 3 mm and 5 mm were modelled as shown in Figure 1 for machining. This profile was modelled and simulated in CNC software called ELCAM. The software generates NC codes in the form of .WC files for the required machining conditions. This .WC file is loaded in Electronica ‘ELPLUS 15 CNCWEDM’ where the wire machines the programmed path. Zinc coated copper wire of diameter 0.25 mm was used as an electrode for machining the profile. The deionised water was used as dielectric fluid throughout the investigation. Figure 1(a) shows fixture made of aluminium H9 series was used to tilt the workpiece. The programmed profile was machined at different taper angles namely 0°, 15° and 30° on workpiece placed on a rotational angular plate of fixture. Figure 1(b) shows the different positions of the workpiece during square profiling. The angular plate is anchored at a specific angle with the help of the slots provided in the side plate. The whole setup with workpiece was mounted on the WEDM table for profiling during the study. As the taper angle increases the slant height(t) also escalates increasing the thickness of cut as observed from Figure 1.

2.3. Characterisation procedure

The machining speed was recorded from the WEDM setup and calculated as the average of all machining/cutting speed at every instant during profiling. The ‘Mitutoyo SJ-301’ made surface roughness tester was utilised for machining roughness measurement. It was recorded an average of 5 machining roughness values of each taper square component. For taper machined errors and recast layer thickness images obtained from ‘JEOL JSM-6368OLA’ and ‘Hitachi SU 3500’ scanning electron microscope (SEM) at 100X and 500X

Table 1. Chemical composition of Hastelloy X superalloy.

%	C%	Si%	Mn%	P%	S%	Cr%	Mo%	Fe%	Co%	W%	Ni%
Composition	0.06	0.21	0.65	0.027	0.01	20.65	8.24	18.05	0.69	0.29	50.88
Required Composition	0.05–0.15	<1	<1	<0.04	<0.03	20.5–23.0	8–10	17–20	0.5–2.5	0.2–1	50–60

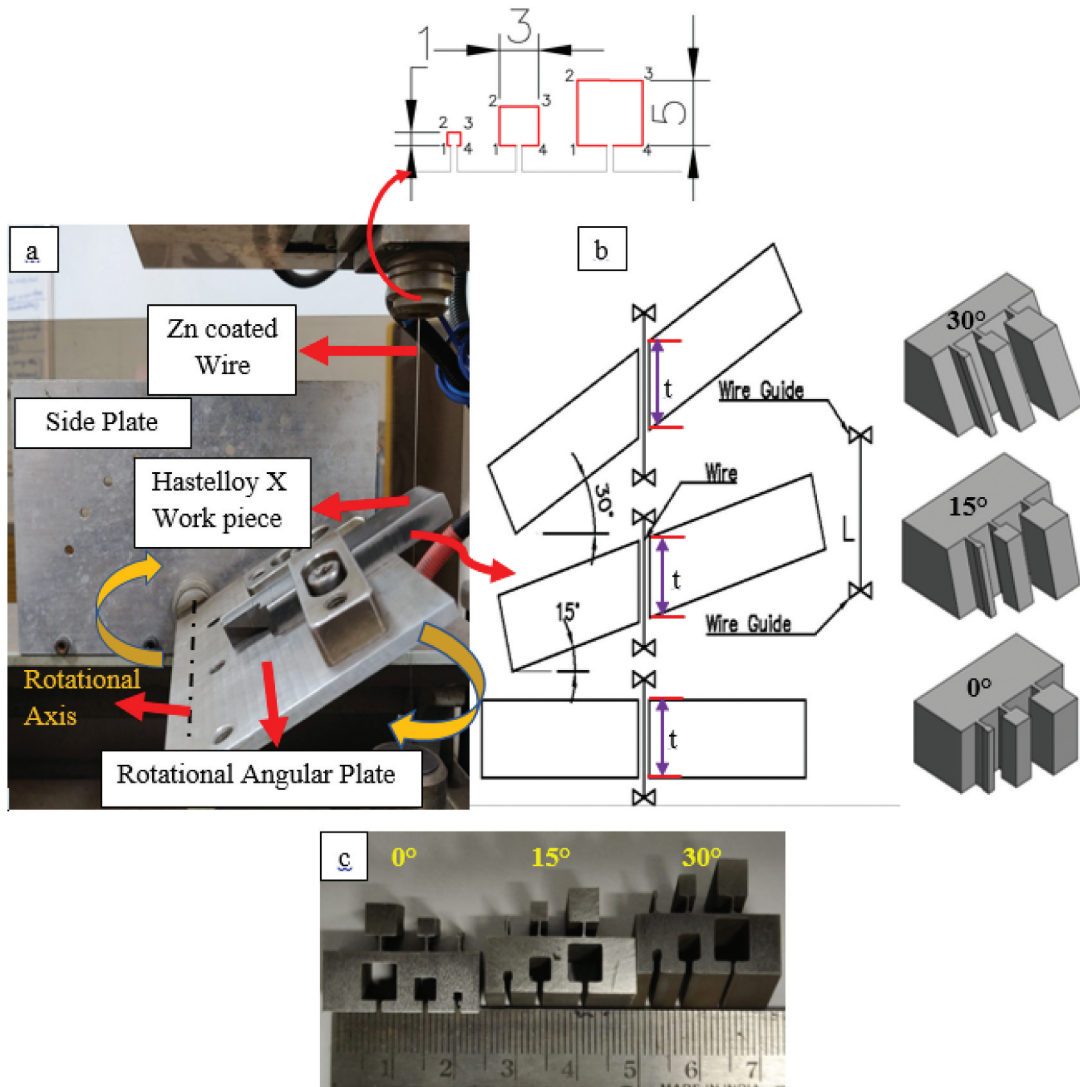


Figure 1. (a) Fixture on WEDM table (b) workpiece position and (c) workpiece at different taper angles.

magnification. Image J software was used to calculate the taper machined error in terms of area for the 2nd corner of profile as shown in Figure 1 and recast layer thickness. The energy dispersive X-ray spectrometry (EDS) was also performed on the machined surface to confirm the metallurgical changes. The effects plots were generated from Minitab software. 'OMNI TECH MVHS-AUTO' make Vicker's micro-hardness tester was used for microhardness. ANN and ANFIS were modelled to predict the machining speed using MATLAB software.

3. WEDM parameters

Table 2 represents both machining parameters and profiling parameters. Based on the initial experiments that were performed the machining parameters were selected. The machining parameters were kept constant throughout the study. The profiling parameters like WDG, CSO, CDT and WO were employed during machining. These parameters were selected on the grounds of machining capability and preliminary

Table 2. WEDM Parameters.

Machining Parameters					
EDM parameters					Settings
Pulse off time (μ s)					44
Servo feed (mm/min)					20
Wire feed (m/min)					6
Pulse on time (μ s)					115
Servo voltage (V)					40
Pulse current (A)					12
Blushing pressure (kg/cm ²)					India Ltd 2011
Corner control (%)					Electronica India Ltd 2011
Profiling parameters					
Wire guide distance (mm)		0°	40	50	60
		15°	75	85	95
		30°	100	110	120
Cutting speed override (%)		31	54	77	100
Wire offset (μ m)		0	40	80	120
Corner dwell time (s)		0	33	66	99

experiments (Electronica India Ltd 2011; Manoj et al. 2019; Manoj, Joy, and Narendranath 2020). The WDG was chosen as such that the profiling could be easily performed with minimal vibration (Electronica India Ltd 2011; Manoj, Joy, and Narendranath 2020). The WDG was found different from initial experiments for all three taper angles as shown in Table 2. Figure 1(c)

shows the different taper square profiles of 10 mm thickness obtained after taper profiling.

4. Results and discussion

4.1. Analysis of machining speed

The variation in machining speed at various parameters for different taper angles is seen in Figure 2. The machining speed was found to be the most influenced by CSO parameter compared to other parameters. It can be observed that the other parameters are constant with slight variations in Figure 2. This phenomenon was seen due to machining errors during profiling. From the effect plots, it can also be highlighted that the machining speed escalates as the CSO percentage increases. The CSO parameter is an on-line parameter that varies the machining speed to the set percentage without modifying the parameters. This parameter can be used for machining complex profiling, tapering, for corners, etc., without wire breakage (Electronica India Ltd 2011; Manoj et al. 2019). The highest machining speed of 1.718 mm/min, 1.628 mm/min and 1.468 mm/min was recorded at 100% CSO and the lowest machining speed was 0.769 mm/min, 0.723 mm/min and 0.695 mm/min noted at 0% CSO for different taper angles respectively irrespective of their dimensions. The effect plots Figure 2 (d) shows a small variation in the increase was observed at 54% and 77% of CSO parameter. This variation was noticed as a result of the wire vibrations caused occurred due to sparking in the wire (Habib 2017). It can be observed that for all the parameters, 0° taper angle yields the highest machining speed and the 30° taper angle showed the least machining speed. The same trend was followed throughout the trials during profiling as shown in Figure 2. This is due to the increased job height with an increase in the taper

angle. For each parameter, the discharge energy remains constant. As the job height increases, more discharge energy and time was required to melt the material. This causes a decrease in the rate of length of cut, in turn reducing the machining speed during profiling (Manoj et al. 2019; Manoj, Joy, and Narendranath 2020).

5. Analysis of machining roughness

Figure 3 and table 3 illustrates the behaviour of machining roughness and different contributing factors of machining parameters. It was noticed from the effects plot that the CSO parameter is the most significant input parameter on the machining roughness. The CDT parameter was the least influential factor on machining roughness compared to other parameters as observed in effects plot and ANOVA. It can be established that the CDT parameter has a very low contribution of 0.3–0.82% on the machining roughness. There were certain minute variations of increase and decrease in the trend of machining roughness, this was due to machining errors during profiling. The CDT parameter can be used to get sharp corners during profiling where the uncut area at corners gets removed (Electronica India Ltd 2011).

5.0.1. Effect of CSO parameter on machining roughness

The CSO parameter controls the discharge energy during machining. It mainly aids in the machining of corners without wire breakage, poor machining conditions, etc. It is a real-time parameter that adjusts itself based on the profile shapes (Electronica India Ltd 2011; Sanchez et al. 2007). As the CSO parameter escalates the machining speed also increases. This increase in machining speed was because of the increase in discharge energy (Manoj et al. 2019). As

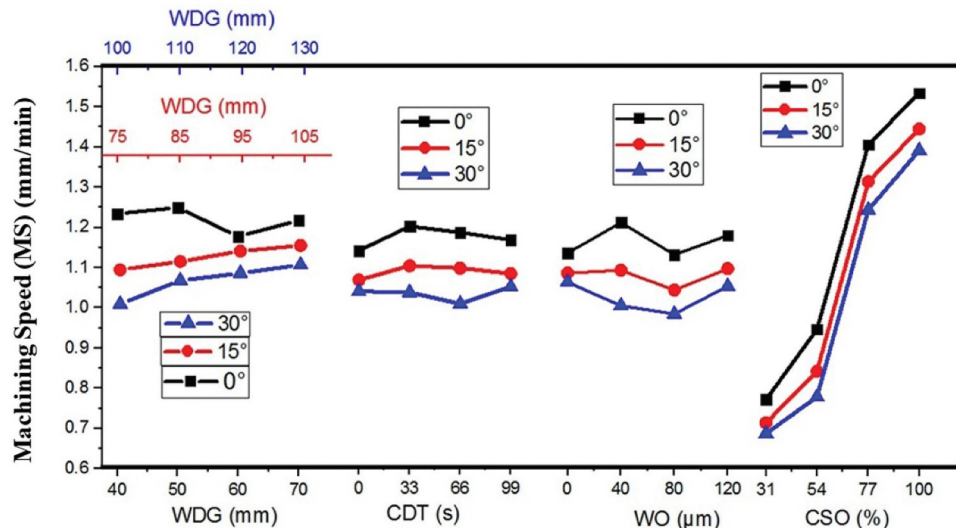


Figure 2. Effects plots for machining speed at different taper angles.

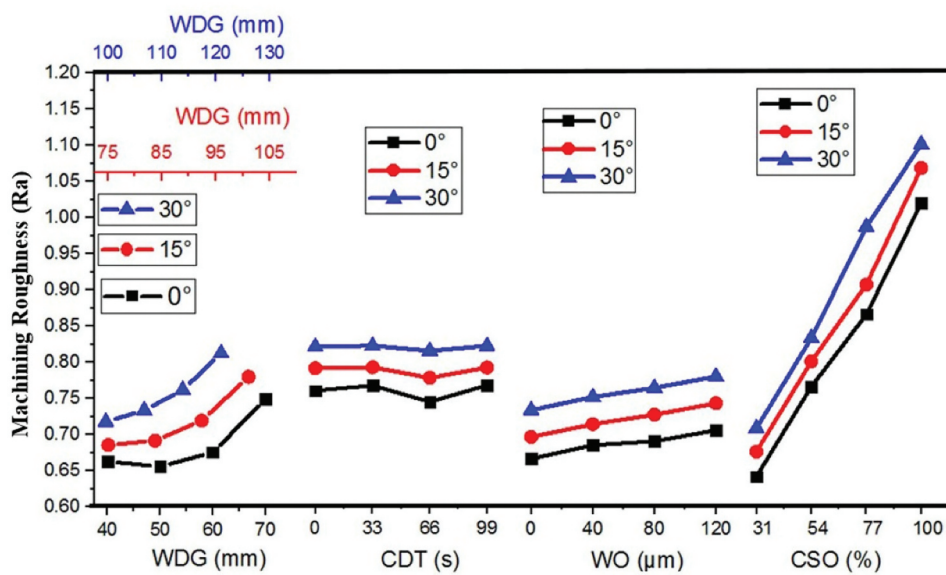


Figure 3. Effects plots for machining roughness at different taper angles.

Table 3. ANOVA for machining roughness at different slant angles.

Sl. No.	Factor	DF	Adj SS	Adj MS	F-Value	P-Value	%Contribution
0° Slant angle							
1	WDG (mm)	3	0.0716	0.0239	2.63		0.224
0.0011		2	0.12	0.945			0.0032
3	CDT (s)	3	0.818				
5.473	WO (μm)	3	0.0214	0.0071	0.79		0.576
4	CSO (%)	3	0.2675	0.0892	9.82		0.046
0.0091		5	Error				0.0272
6	Total	15	0.3910				
15° Slant angle							
1	WDG (mm)	3	0.0492				0.0164
1.95		2	0.298				12.275
2	CDT (s)	3	0.0014				0.0005
0.06		3	0.979				0.349
3	WO (μm)	3	0.0176				0.0059
0.70		3	0.612				4.391
4	CSO (%)	3	0.3073				0.1024
12.19		3	0.035				76.672
5	Error	3	0.0252				0.0084
6	Total	15	0.4008				
30° Slant angle							
1	WDG(mm)	3	0.0592	0.01975		0.382	11.506
2	CDT (s)	3	0.0002	0.00005	1.46	1.000	0.039
3	WO (μm)	3	0.0309	0.01031	0.00	0.586	6.006
4	CSO (%)	3	0.3835	0.12784	0.76	0.049	74.538
5	Error	3	0.0407	0.0136	9.43		
6	Total	15	0.5145				

the discharge energy increases the intensity of sparks also increases. This increases the sparks hitting the machined surface and melting of the workpiece. Due to higher discharge energy the craters, partially melted

surface with micro globules, modules, holes and metal debris, cracks etc. will increase. This causes higher peaks and valleys which increases the machining roughness (Manoj, Joy, and Narendranath 2020).

This escalates the machining roughness as the CSO parameter increases with can be seen in the effect plots in [Figure 3](#). A small variation in the increase was observed caused due to the wire vibration due to the sparking ([Habib 2017](#)).

5.0.2. Effect of WDG parameter on machining roughness

The WDG parameter controls the wire distance between the guides. As WDG increases the wire span between the guides also escalates ([Electronica India Ltd 2011](#)). This increase in wire span decreases the wire tension. The decreases in the wire tension cause wire deflection/lag in machining ([Chen et al. 2018](#)). Chaudhary et al ([Chaudhary, Siddiquee, and ChandaA. 2019](#)) stated that with the increase in wire tension the vibration of the wire reduces, which leads to a decrease in the machining roughness. As the tension in the wire increases between the guide span, the wire vibration was reduced. In the case of higher WDG parameter due to lower wire tension, there were more vibrations due to sparking. This causes irregular sparking which increases the machining roughness. This phenomenon is observed in [Figure 3](#) so as the WDG parameter increases the machining roughness also increases. In [Figure 3](#) there are variations in increases due to the change in wire tension as wire span increases. As the wire tension varies the wire vibration also gets affected ([Habib 2017; Chaudhary, Siddiquee, and ChandaA. 2019; Puri and Bhattacharyya 2003a](#)). The WDG contributed 11.51–18.31% to machining roughness.

5.0.3. Effect of WO parameter on machining roughness

WO parameter contributes 68.41–76.67% to the machining roughness. The WO parameter defines the distance between the machined profile and the programmed profile. This provides the offset distance for the wire so that the profile can be both bigger/smaller to the programmed profile. This distance can be fixed by part programming ([Electronica India Ltd 2011](#)). [Habib and Okada \(Habib and Okada 2016\)](#) stated as the wire offset escalates, the wire will machine a larger profile circumference than the programmed profile. This leads to a reduction in the wire vibration so the machining speed escalates. This increases the values of peaks and valleys, thus increasing the machining roughness ([Manoj, Joy, and Narendranath 2020](#)). This phenomenon can be observed in effect plots in [Figure 3](#). It was noticed a small variation in increase, this was due to the machining errors caused during profiling. There is a small increase in variations at 80 µm as seen in [Figure 3](#). These are due to machining errors during profiling.

5.1. Variation of machining roughness at various taper angles and machining speed

The machining roughness behaviour for different taper angles can be seen in [Figure 4](#). The machining roughness increases although the machining speed decreased. A contrasting scenario was observed in case of taper machining. The machining speed decreased with escalating taper angle as a result of the increase in job height/thickness ([Manoj et al. 2019; Manoj, Joy, and Narendranath 2020](#)). As the discharge energy remains constant for a parameter, an increase in job height/thickness decreases the machining speed as stated in [section 3](#). The machining roughness escalates as the taper angle increases as a result of the increase in job height. Hence, the surface exposed to the sparking also increases ([Manoj, Joy, and Narendranath 2020](#)). This increases the craters, partially melted surface with a larger number of smaller micro globules, modules, holes etc. which increases the peak and valleys resulting in higher machining roughness as shown in [Figure 4](#). It shows lesser craters, micro globules, modules, holes etc. which was cut at 0°angle with the highest machining speed. So there is a contrasting behaviour of machining roughness increasing although the machining speed decreases. This clearly shows the increase in machining roughness with machined taper angles.

5.2. Recast layer thickness and microhardness of tapered components

[Figure 5](#) shows the recast layer for various taper components. For a specific parameter, at highest and lowest machining speeds the recast layer thickness decreases as the taper angle increased. This was due to the increase in job height which increases the taper angle. The discharge energy for a specific parameter remains constant. As the taper angle increases, the discharge energy during machining also gets distributed due increase in job height ([Manoj, Joy, and Narendranath 2020; Manjaiah and Rudolph 2017; Joy, Manoj, Narendranath 2020](#)). Therefore the recast layer thickness gets smaller as the taper angle increases. The microhardness was measured as shown in [Figure 6 \(a\) and \(b\)](#) on the same cross-section of WEDMed surface. It was observed that at both highest and lowest machining speed the hardness at the machined surface was lower than the base metal. As the distance from the machining surface increases the hardness returns to the base metal value. This change was observed due to the thermal degradation in the machined surface ([Abyar, Abdullah, and Shafaroud 2019](#)). It can be seen that as the taper angle increased, the hardness also increased due to the lower thermal degradation. The discharge energy gets distributed as the taper angle increased leading to

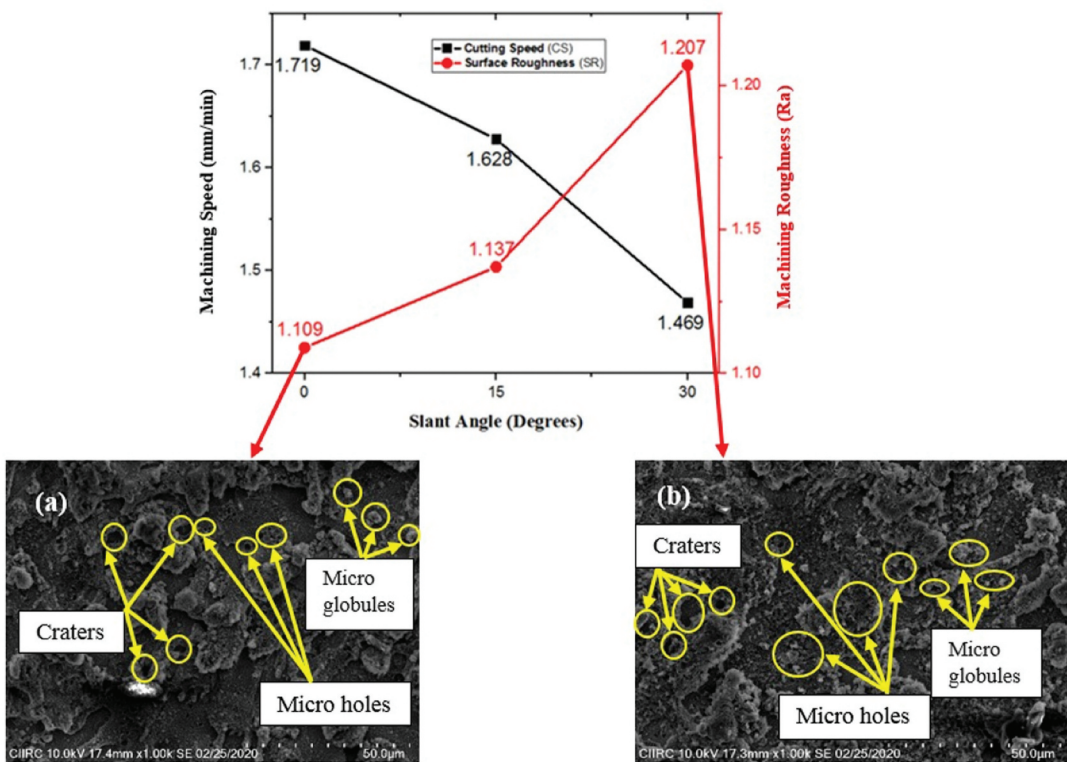


Figure 4. Variation of surface roughness with machining speed and SEM images of WEDMed surface at taper angle (a) 0° and (b) 30°.

the lower thermal degradation (Manjaiah and Rudolph 2017). The EDS images in Figure 7 (a) and (b) shows that the degradation in the material was due to the presence of O, Zn and Cu in the nickel superalloy. The Zn and Cu diffused into the base metal through the zinc-coated copper electrode and O due to dielectric water used for machining.

5.3. Analysis of taper machined error

Machining error is the uncut material on the corners of the profile due to wire deflection. From Figures 8, 9Table 4, it can be seen that WDG is the most contributing and influential factor with 65.62–55.31%. It was followed by WO and CSO parameters. The CDT parameter had the least influence in the ANOVA table with error ranging from 1.12–1.77%. The CDT is a corner machining parameter that controls the uncut material in corner. It depends on the angle, machining speed and profile that is machined (Electronica India Ltd 2011). It was observed that CDT parameter influenced for lower angles.

5.3.1. Influence of WDG parameter on taper machined error

The WDG parameter is the wire distance between the guides that were varied during profiling. As WDG increases the wire span also increases which reduces the tension in the wire. This parameter accommodates machining of various complex surfaces like different

job thickness, complex profiles, tapering, etc. (Electronica India Ltd 2011). It can be observed from the effect plots, it was the most influential factor on machining error for all taper angles. As the WDG increases the machining error also increased for all the profile irrespective of dimensions. This effect was observed due to the wire lag/deflection phenomenon that occurs during machining (Chen et al. 2018). As the wire distance between the guides widened, the wire span also escalated. This leads to an increase in wire length/span during profiling causing wire lag/deflection (Sanchez et al. 2007). A clear increasing trend of machining error can be witnessed in Figure 9(a). There are small variations for different taper angles i.e. at 60 mm, 95 mm and 120 mm for respective taper angles. This slight variation occurs because of the stochastic wire vibration instigated by increased wire span between the guides (Puri and Bhattacharyya 2003a, 2003b).

5.3.2. Influence of WO parameter on taper machined error

WO parameter gives an offset to the wire that leads to increase dimensions (area) of programmed profile that was fed to the machine. It is used as a compensation parameter for overcut/undercut of the profile (Electronica India Ltd 2011). From the effect plots in Figure 9(b), we can notice as WO parameter increases the machining error also escalates. This effect was caused by the deflection in the wire (Chen et al.

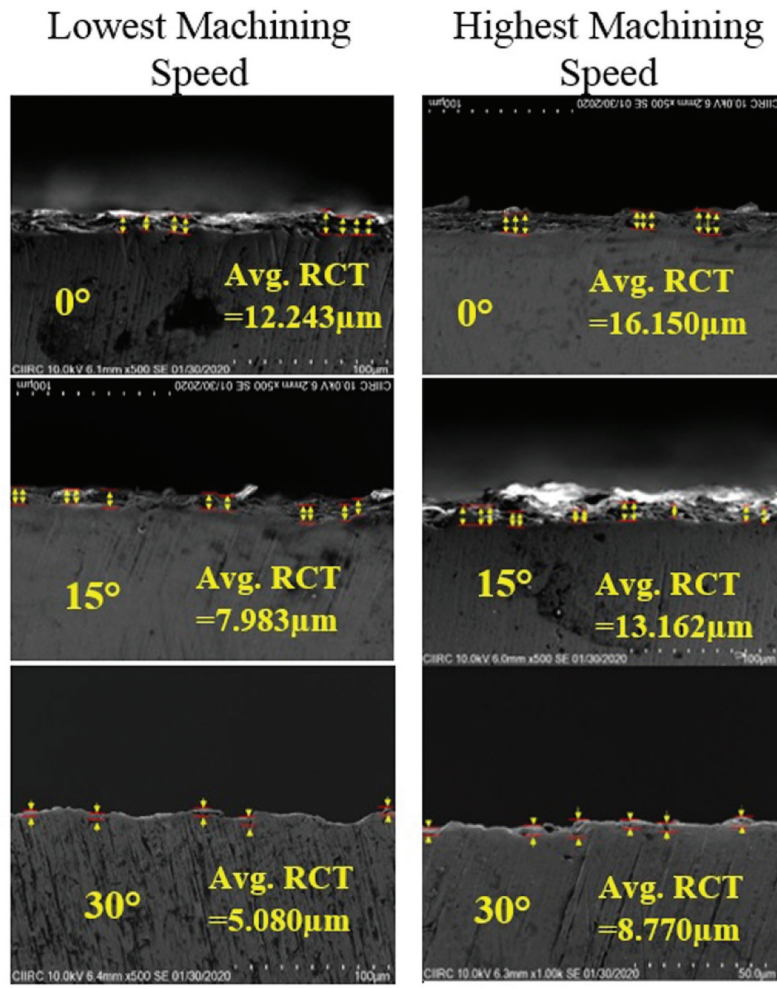


Figure 5. Recast layer thickness at different taper angles.

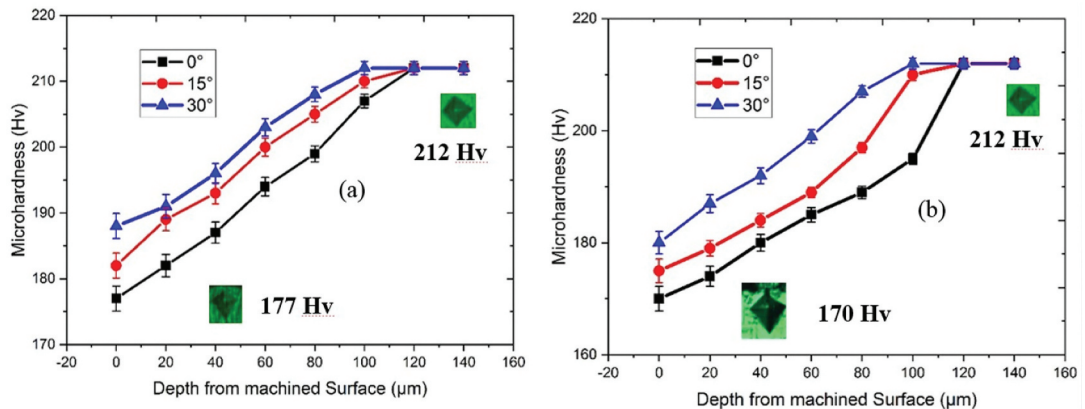


Figure 6. Micro-hardness at different taper angles for (a) lowest and (b) highest machining speeds.

2018). As the WO parameter increases, the wire cut path becomes larger, having to machine a larger area than the profile circumference which leads to increase in wire deflection (Habib and Okada 2016). From the

Figure 9(b) there can be a small variation of increase observed in 40 μm and 80 μm for all the taper angles. These small variations were due to vibrations at the time of profiling (Puri and Bhattacharyya 2003a).

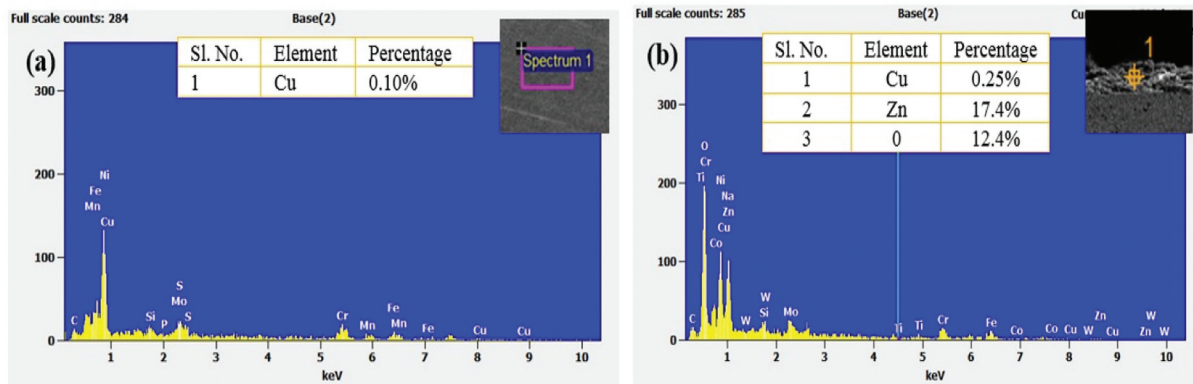


Figure 7. EDS images of (a) before machining (b) after machining through WEDM.

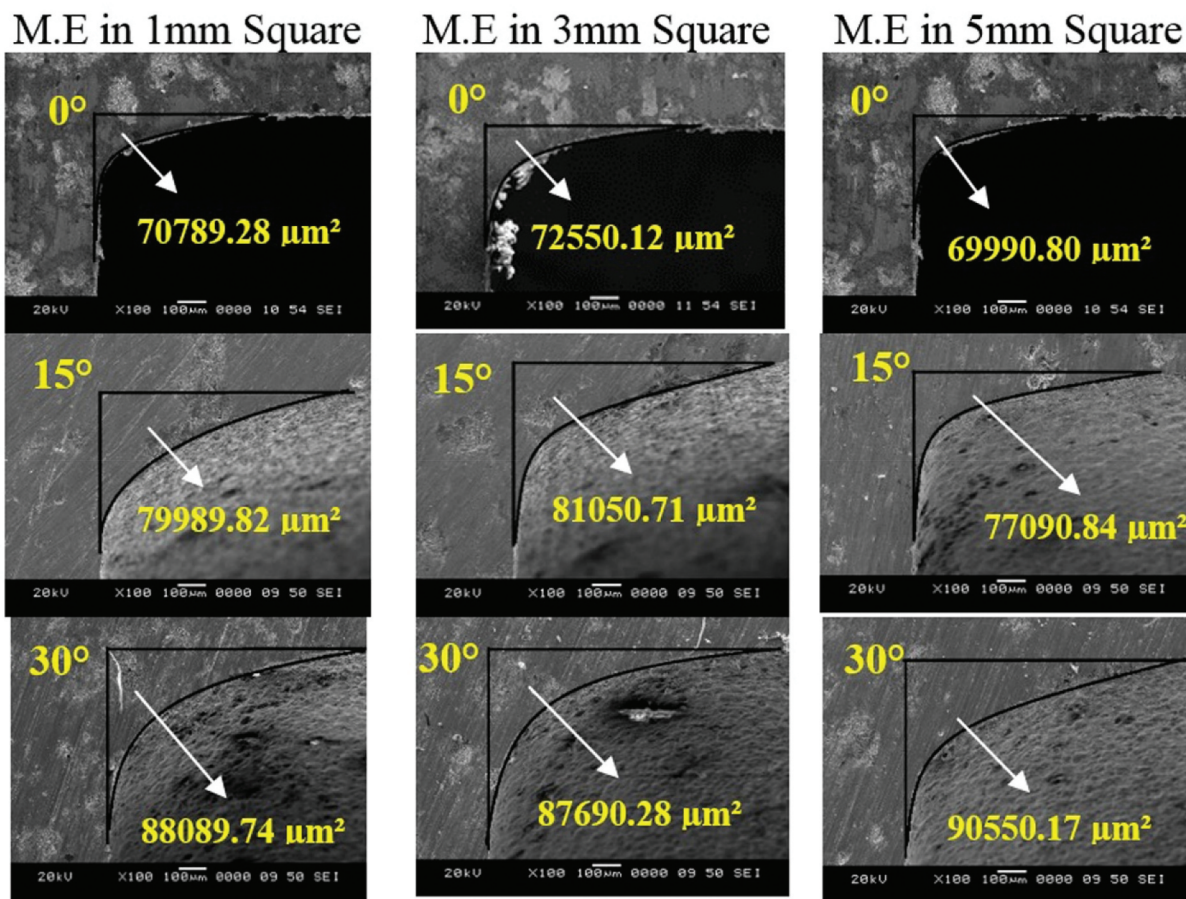


Figure 8. SEM images of machining error at the corners (M.E.).

Machining error also depends on factors like job height, corner angles, and the profile that has to be machined (Sarkar et al. 2010; Puri and Bhattacharyya 2003b).

5.3.3. Influence of CSO parameter on tapered machined error

The CSO is an operational parameter that controls the discharge energy during cutting without varying machining parameter (Electronica India Ltd 2011; Manoj et al. 2019). Figure 9(c) demonstrates the escalation in machining error as the CSO parameter

increases. This effect was caused by the increase in wire deflection/lag (Habib and Okada 2016; Selvakumar, Jiju, Sarkar, Mitra 2016). There was a clear escalation in machining error as the CSO % increases, in 5 mm square at 15° taper angle. Slight variations in the increase were noticed at 77% of CSO parameter at all the taper angles. This occurrence was because at the higher machining speed (higher CSO parameter) leads to an increase in wire vibrations (Bisaria and Shandilya 2019; Sarkar et al. 2010). Due to the chaotic nature of wire vibration, these small variations were observed in effect plots.

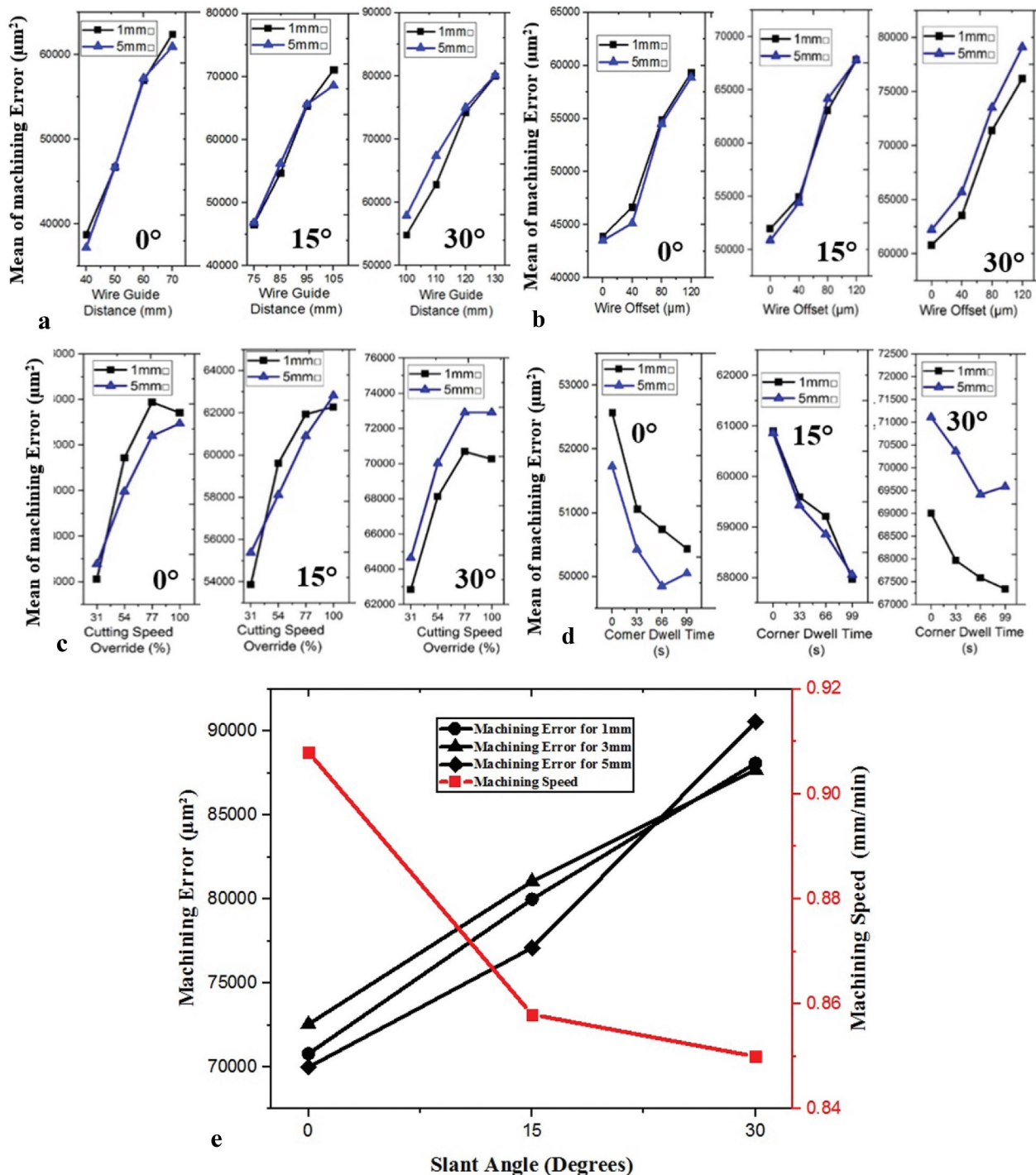


Figure 9. Variation of machining error at different (a) WGD (b) WO (c) CSO (d) CDT and (e) taper angles and machining speed.

5.3.4. Influence of CDT parameter on taper machined error

From the effects plot, as the CDT increases, the machining error decreases due to the decrease in wire lag. The corner dwell time (CDT) stops the profiling operation at specific co-ordinate for the period (Electronica India Ltd 2011). The wire guide stops at that co-ordinate which will give the wire time to travel to the point, avoiding the lag. Hence, reducing the undercut decreasing the

machining error to achieve sharper corners (Chen et al. 2018; Selvakumar, Kuttalingam, and Prakash 2018). This effect can be seen in 5 mm, 1 mm squares at 15° and 30° taper angles as shown in Figure 9 (d). Small variations of decrease were observed at 66 sec for different profiles. This was due to the wire vibration during machining dwell time at corners. The change in forces on the wire caused at the time of sparking and discharging makes the wire to vibrate (Sarkar et al. 2010).

Table 4. ANOVA table for corner error.

Sl. No.	Factor	DF	Machining Error in 1 mm		Machining Error in 3 mm		Machining Error in 5mm	
			Sum of squares	% Contribution	Sum of squares	% Contribution	Sum of squares	% Contribution
0° Slant angle								
1	WDG	3	1,334,419,152	62.27	1,148,527,728	55.13	1,382,321,044	63.40
2	CDT	3	10,785,780	0.50	12,254,291	0.59	8,536,116	0.39
3	WO	3	613,907,714	28.65	719,334,749	34.53	655,723,533	30.07
4	CSO	3	152,314,799	7.11	177,558,612	8.52	95,033,847	4.36
5	Error	3	31,676,496	1.48	25,585,721	1.23	38,693,987	1.77
15° Slant angle								
1	WDG	3	1,440,236,734	62.51	1,078,512,198	49.82	1,167,612,363	55.31
2	CDT	3	17,546,723	0.76	15,285,561	0.71	16,746,280	0.79
3	WO	3	638,838,853	27.73	846,666,525	39.11	762,746,562	36.13
4	CSO	3	181,782,504	7.89	198,835,595	9.18	127,086,898	6.02
5	Error	3	25,699,964	1.12	25,647,027	1.18	36,749,753	1.74
30° Slant angle								
1	WDG	3	1,525,557,882	65.62	1,120,169,236	58.36	1,127,123,375	55.32
2	CDT	3	6,442,480	0.28	12,254,212	0.64	7,285,776	0.36
3	WO	3	602,946,539	25.94	653,142,831	34.03	697,676,704	34.24
4	CSO	3	155,908,558	6.71	102,068,577	5.32	182,123,250	8.94
5	Error	3	33,886,413	1.46	31,618,761	1.65	23,298,905	1.14

5.4. Variation of taper machined errors for the highest machining speed at different taper angles

Figure 9 (e) shows the behaviour of machining speed and machining error with different taper angles during square profiling. Figure 8 illustrates the machining error that was recorded by SEM at the highest machining speed for various taper angles. It can be witnessed that the machining speed decreases as the taper angle escalates due to the increase in job thickness. It was stated by Selvakumar et al (Selvakumar, Kuttalingam,

and Prakash 2018) as the machining error escalated as the profile was machined at the increasing machining speed which was found to be contrasting in case of slant type taper profiling. The machining error increased with increase in taper angle although the machining speed got decreased. This phenomenon was due to the escalation in job thickness (Zhang et al. 2016). The wire lag effect/wire deflection increased with the escalation of the job thickness. So the uncut region also increases due to the increased

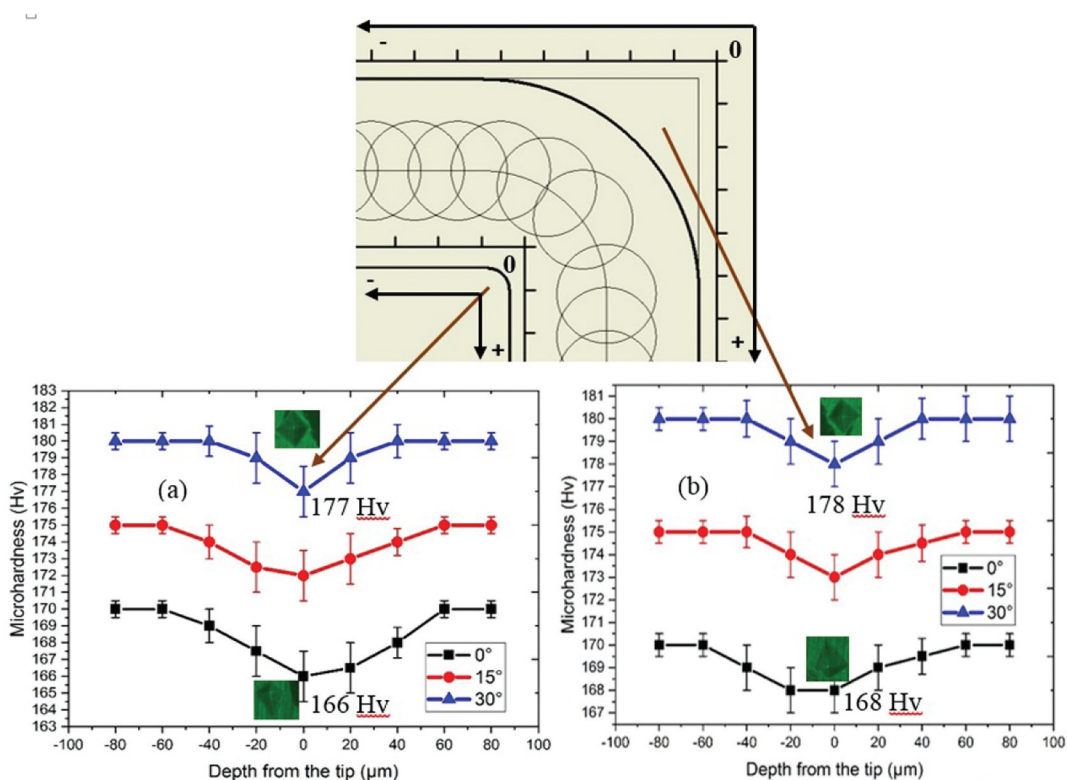


Figure 10. Variation of microhardness at (a) inner and (b) outer corners for different taper angles.

wire lag causing machining error (Chen et al. 2018; Puri and Bhattacharyya 2003a).

5.5. Variation of microhardness at tapered corners

Figure 10 shows the microhardness of both inner and outer corners that were recorded for the profile machined at highest machining speed. It was observed that the strength of the corner was reduced as it was affected due to the discharge energy. The heat generated due to the discharge energy causes thermal degradation of the material (Abyar, Abdullah, and Shafaroud 2019). The CSO parameter controls the discharge energy without changing the machining parameter during profiling. The discharge energy controls the machining speed helping in corner formation during machining (Electronica India Ltd 2011; Manoj et al. 2019; Sanchez et al. 2007). It was observed that the straight edges of the profile are cut at different machining speed than the profile corners. The CSO parameter aids during complex and taper profiling without wire breakage and corner damage (Electronica India Ltd 2011). The CSO parameter optimises the discharge energy which controls the machining speed (Manoj et al. 2019). This helps in the formation of the sharp tapered corners (Electronica India Ltd 2011; Sanchez et al. 2007). So the corner was always observed to be softer compared to the edges. It was observed that the inner corners were softer than the outer corners. This was because outer corners have larger circumference which leads to better heat distribution and faster cooling (Manjaiah and Rudolph 2017; Sarkar et al. 2010).

5.6. Prediction of machining speed using ANN and ANFIS models

Table 4 shows the different parameters utilised for the optimal model. There were 16 experiments conducted for each taper angle and 48 iterations were considered for training, validation and testing for both the models. The input parameters were WDG, WO, CDT, WO, and taper angle during square profiling. The taper angle was also considered as an input as it was observed from section 5.5 and 4.4 that it influences the machining speed. The combination of the Levenberg-Marquardt (LM) algorithm and back propagation neural network (BPNN) is most effective in production as reported by Gosh et al (Raj, S. and Prabhu 2017; Manoj and Narendranath 2019) similar model were considered. The output (machining/cutting speed) were normalised from 1 to -1 during training, validation and testing. For the neural network considered there are 1 input layer, 1 hidden layer and output layer. The layers can be represented as

$$O_i = U_1(O_{ij}X_i + a_{ij}) \quad (1)$$

(Kara, Aslantas, and Çiçek 2016)

Where, O_i are the outputs of the first layer (input), U_1 is the tan-sig transfer function, O_{ij} are the weights from the input layer, X_i is the input of the input layer, a_{ij} is the biases of the first hidden layer. $i=1,2,3, 4$ and $j=1,2,3, 4$

$$Z_m = U_2(O_{km}V_k + a_{km}) \quad (2)[32]$$

Where, Z_m are the outputs of the hidden layer, U_2 is the pure-line transfer function, O_{km} are the weights from hidden layer k to output layer m, V_k is input from the preceding layer, a_{km} is the biases of the output layer.

The ANFIS model was modelled using five network layers. As stated by Maher et al (Maher et al. 2016) and by carrying different trials, it was concluded that the Gaussian membership function tabulates the least errors. (No. of epochs 500 and output function used was constant). Among the parameters, the ratio of 80% of the date was considered for training the model and 10% were considered for the testing model. This ratio gave the lowest testing errors. There were 5 network layers used each network layer was assigned two membership function. The training to testing ratios, type and number of membership function were assigned based on different trials carried out during building the model. The system includes five inputs r_1, r_2, r_3, r_4 and r_5 the output U_1 and the rule base contains fuzzy rules which can be expressed by

$$U_1 = m_1r_1 + n_1r_2 + o_1r_3 + p_1r_4 + r_5 \quad (3)[34]$$

and so on. Where m_i, n_i, o_i and p_i are the linear parameters. $i=1, 2, 3, 4 \dots$ and $j=1, 2, 3, 4 \dots$

$$Q_i = \sum_i \bar{w}_i U_i = \frac{\sum_i w_i U_i}{\sum_i w_i} \quad (4)$$

Table 5. Optimal model details.

Sl. No.	Network parameters	Values
Artificial Neural Network		
1	Network structure	5-8-1-1
2	Total number of training/ validation/testing data sets	32/8/8(48 experiments)
3	Network algorithm	Feed forward backpropagation
4	Type of transfer function	Tangential sigmoid
5	Type of training function	TRAINLM
6	Learning function	LEARNGDM
7	Performance function	MSE
Adaptive Neuro Fuzzy Inference System		
1	Total number of inputs	48
2	Total number of outputs	1
3	Total number of training/testing data sets	38/10
4	Type of input membership function	Gaussian
5	Type of output membership function	Constant
6	Total number of fuzzy rules	32 rules
7	Number of epochs	500/output

Table 6. Predicted and measured areas of triangles at different taper angles.

Taper Angle (Degree)	Sl. No.	WDG (mm)	CDT (s)	WO (μm)	CSO (%)	Machining Speed in mm/min		
						ANN	ANFIS	Experimental
0°	1	40	0	0	31	0.785	0.769	0.769
	2	40	33	40	54	1.099	1.126	1.126
	3	40	66	80	77	1.417	1.392	1.427
	4	40	99	120	100	1.596	1.616	1.616
	5	50	0	40	77	1.496	1.501	1.501
	6	50	33	0	100	1.593	1.599	1.599
	7	50	66	120	31	0.892	0.898	0.898
	8	50	99	80	54	1.009	1.001	1.000
	9	60	0	80	100	1.562	1.558	1.558
	10	60	33	120	77	1.536	1.523	1.523
	11	60	66	0	54	0.891	0.889	0.889
	12	60	99	40	31	0.721	0.719	0.739
	13	70	0	120	54	0.936	0.908	0.908
	14	70	33	80	31	0.733	0.749	0.749
	15	70	66	40	100	1.720	1.718	1.718
15°	16	70	99	0	77	1.500	1.495	1.495
	17	75	0	0	31	0.743	0.693	0.723
	18	75	33	40	54	0.895	0.876	0.876
	19	75	66	80	77	1.295	1.289	1.289
	20	75	99	120	100	1.519	1.490	1.490
	21	85	0	40	77	1.352	1.345	1.345
	22	85	33	0	100	1.545	1.507	1.507
	23	85	66	120	31	0.764	0.754	0.754
	24	85	99	80	54	0.846	0.901	0.855
	25	95	0	80	100	1.498	1.493	1.493
	26	95	33	120	77	1.465	1.479	1.479
	27	95	66	0	54	0.875	0.872	0.876
	28	95	99	40	31	0.712	0.715	0.705
	29	105	0	120	54	0.859	0.858	0.858
	30	105	33	80	31	0.712	0.708	0.718
30°	31	105	66	40	100	1.628	1.628	1.628
	32	105	99	0	77	1.420	1.513	1.427
	33	100	0	0	31	0.694	0.681	0.695
	34	100	33	40	54	0.706	0.718	0.718
	35	100	66	80	77	1.158	1.160	1.160
	36	100	99	120	100	1.463	1.467	1.467
	37	110	0	40	77	1.302	1.297	1.297
	38	110	33	0	100	1.508	1.527	1.499
	39	110	66	120	31	0.697	0.698	0.698
	40	110	99	80	54	0.774	0.779	0.779
	41	120	0	80	100	1.446	1.449	1.449
	42	120	33	120	77	1.372	1.370	1.369
	43	120	66	0	54	0.834	0.819	0.834
	44	120	99	40	31	0.701	0.693	0.693
	45	130	0	120	54	0.860	0.856	0.856
	46	130	33	80	31	0.715	0.658	0.698
	47	130	66	40	100	1.469	1.468	1.468
	48	130	99	0	77	1.418	1.406	1.406

2019 Where Q_i is the overall output, \bar{w}_i is the output of (layer 3), U_i is fuzzy rules.

It can be observed from Tables 5 and 6 that the ANFIS was more accurate than ANN. The average percentage error for the ANFIS model (0.57%) was also lesser than the ANN model (0.83%). The optimal ANN and ANFIS model were validated experimentally

in Table 5. The ANFIS model is obtained to be more accurate than the ANN model.

5.6.1. ANFIS model mapping

From the ANFIS model, the input and output relationship was obtained as shown in Figure 11 obtained from MATLAB. It shows a three-dimensional variation of machining speed with three taper angles for different investigating parameters. The ANFIS mapping shows that the machining speed was most affected by the CSO parameter as obtained from effects plot as in Figure 2. The mapping also clearly shows that with the escalation of taper angle there was a decrease in machining speed as stated in section 3. It can also be observed that the WDG and CDT have a very low effect on machining speed. From Figure 11 (d) it can be concluded that the machining speed increases as WO parameter increases. The WO parameter escalates the vibrations of the wire becomes limited. This increases the machining speed due to lower wire vibration stated as by Habib and Okada (Habib and Okada 2016) which were not traced in case of effects plots as in Figure 2.

6. Conclusion

The taper square profile of 0°, 15° and 30° were machined using WEDM with the aid of a novel fixture. Different input parameters like WDG, WO CDT and CSO were investigated on profiling response characteristics. Based on the above investigation the following conclusions can be drawn Table 7.

(Naresh Chakala, Chandrabose, and Rao 2019). From the effects plot the cutting speed override CSO parameter influences both machining speed and machining roughness of the profile. As CSO increases the machining speed also increases by 106.31–111.40% and machining roughness increase by 56.32–63.56%

(Raj, S. and Prabhu 2017). In case of machining error, the WDG parameter is the most influencing parameter. As WDG increases, the machining error also increased from 45.77–61.019%. The parameters yielding minimal errors were WDG = 40 mm for 0°, 75 mm for 15° and 100 mm for 30°, CDT = 99s, WO = 0 μm and CSO = 31% based on machining parameters.

(Somvir, Dixit, and Kumar 2018) As the component angle escalates from 0° to 30°, the machining

Table 7. Experimental, ANN and ANFIS predicted machining speeds.

Sl. No.	WDG (mm)	CDT (s)	WO (μm)	CSO (%)	Taper Angle (Degree)	Machining Speed in mm/min				
						Measured	ANN Predicted	Error %	ANFIS Predicted	Error %
1	55	40	100	45	0°	0.86	0.848	1.41	0.875	1.10
2	65	55	80	55	0°	1.08	1.026	5.00	1.180	2.00
3	90	50	75	65	15°	1.20	1.109	7.58	1.540	4.48
4	80	70	55	95	15°	1.47	1.326	9.77	1.370	1.02
5	115	80	50	90	30°	1.30	1.267	2.42	1.354	2.31
6	125	40	30	80	30°	1.28	1.236	3.46	1.250	0.87

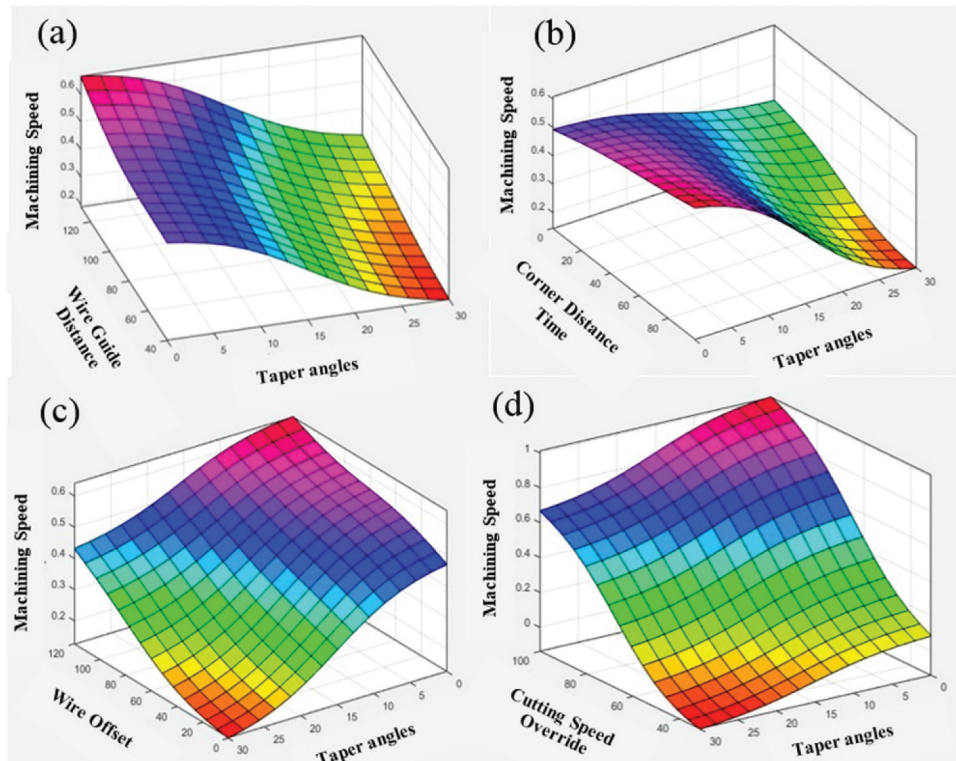


Figure 11. Variation of the machining speed for different input parameters and taper angle.

speed is found to decrease by 14.54%, the machining roughness is found to increase by 8.84% and the machining error increased from 20.87–29.37% for highest machining speed parameter.

[4] Recast layer thickness decreased by 58.49–45.69% as the taper angle increased from 0° to 30°. This is observed due to the increase in job height which leads to a better distribution with low thermal degradation due to discharge energy.

(Abyar, Abdullah, and Shafaroud 2019) The micro-hardness at WEDMed surface is observed increased from 1.61–5.88% as the taper angle escalated from 0° to 30°. It is found by EDS that the hardness decreased at the machined surface due to the presence of O, Cu and Zn. It is also observed that the inner corners (166Hv) were softer than the outer corners (168Hv).

(Abyar, Abdullah, and Akbarzadeh 2018) Both ANN and ANFIS model was modelled to predict the machining speed. The ANFIS model gives the least error for both experimental and validation parameters. The WO parameter also influenced the machining speed as noticed in ANFIS input-output mapping which is not highlighted in the effects plots.

Data availability statement

The authors confirm that the data supporting the findings of this study are available within the article [and/or] its supplementary materials.

Thank you,
I.V.Manoj
S.Narendranath

Disclosure statement

No potential conflict of interest was reported by the author(s).

Notes on contributors

I.V.Manoj is a PhD research scholar under Dr Narendranath. S from the National Institute of Technology, Surathkal, and Karnataka. He completed his Masters of Technology in Product Design and Manufacturing from R.V. College of Engineering, Bangalore, Karnataka, India. He completed his Bachelors of Engineering in Mechanical Engineering from Acharya Institute of Technology, Bangalore, Karnataka, India.

Dr. Narendranath S is a professor at National Institute of Technology, Surathkal, and Karnataka for 24 years. His main areas of research are Non-Traditional Machining of advanced materials, Severe Plastic Deformation Corrosion and Shape Memory Alloys. He has guided 16 PhD students. He did his PhD in 2006 at IIT Kharagpur, West Bengal, India on smart materials. He completed the Masters of Technology at University BDT College of Engg. Kuvempu University, Karnataka on Production Engineering & System Technology. He pursued his bachelor's degree in mechanical at Govt. BDT College of Engg. Mysore University, Karnataka.

References

- Abyar, H., A. Abdullah, and A. Akbarzadeh. 2018. "Analyzing wire deflection error of WEDM processes on small arced corners." *Journal of Materials Processing Technology* 36: 216–223.
- Abyar, H., Abdullah, A., and Shafaroud, A.A. 2019. "Theoretical and experimental analysis of machining errors on small arced corners during WEDM finishing stages." *Journal Machining Science and Technology An International Journal* 23(5): 734–757.
- Bisaria, H., and P. Shandilya. 2019. "Experimental Investigation on Wire Electric Discharge Machining (WEDM) of Nimonic C-263 Superalloy." *Materials and Manufacturing Processes* 34 (1): 83–92. doi:10.1080/10426914.2018.1532589.
- Chandler H. 2006. "Heat Treater's Guide Practices and Procedures for Nonferrous Alloys." Third Printing, ASM International, Materials Park, OH 44073-0002 (Printed in the United States of America).
- Chaudhary, T., A.N. Siddiquee, and K. ChandaA.. 2019. "Effect of Wire Tension on Different Output Responses during Wire Electric Discharge Machining on AISI 304 Stainless Steel." *Defence Technology* 15 (4): 541–544. doi:10.1016/j.dt.2018.11.003.
- Chen, Z., Y. Zhang, G. Zhang, and W. Li. 2018. "Modeling and Reducing Workpiece Corner Error Due to Wire Deflection in WEDM Rough Corner-cutting." *Journal of Materials Processing Technology* 36: 557–564.
- Electronica India Ltd, "Operating Manual for ELPLUS 15 Ecocut, 2011" Retrieved by email from company, access date : 25May 2011.
- Habib, S. 2017. "Optimization of Machining Parameters and Wire Vibration in Wire Electrical Discharge Machining Process." *Mechanics of Advanced Materials and Modern Processes* 3 (1): 1–9. doi:10.1186/s40759-017-0017-1..
- Habib, S., and A. Okada. 2016. "Experimental Investigation on Wire Vibration during Fine Wire Electrical Discharge Machining Process." *The International Journal of Advanced Manufacturing Technology* 84 (9–12): 2265–2276. doi:10.1007/s00170-015-7818-3.
- Joy, R., I.V. Manoj, and S. Narendranath. 2020. "Investigation of Cutting Speed, Recast Layer and Micro-hardness in Angular Machining Using Slant Type Taper Fixture by WEDM of Hastelloy X." *Materials Today: Proceedings* 27: 1943–1946.
- Kara, F., K. Aslantas, and A. Çiçek. 2016. "Prediction of Cutting Temperature in Orthogonal Machining of Aisi 316l Using Artificial Neural Network." *Applied Soft Computing* 38: 64–74. doi:10.1016/j.asoc.2015.09.034.
- Maher, I., A.A.D. Sarhan, H. Marashi, M.M. Barzani, and M. Hamdi. 2016. "White Layer Thickness Prediction in wire-EDM Using Cu Zn-coated Wire Electrode – ANFIS Modelling." *Transactions of the IMF* 94 (4): 204–210. doi:10.1080/00202967.2016.1180847.
- Manikandan, N., K. Balasubramanian, D. Palanisamy, P.M. Gopal, D. Arulkirubakaran, and J.S. Binoj. 2019. "Machinability Analysis and ANFIS Modelling on Advanced Machining of Hybrid Metal Matrix Composites for Aerospace Applications." *Materials and Manufacturing Processes* 34 (16): 1866–1881. doi:10.1080/10426914.2019.1689264.
- Manjaiah, M., and F. L. Rudolph. 2017. "Study on Recast Layer Thickness and Residual Stress during WEDM of SMAs." *Emerging Materials Research* 6 (1): 82–88. doi:10.1680/jemmr.16.00120.
- Manoj, I.V., R. Joy, and S. Narendranath. 2020. "Investigation on the Effect of Variation in Cutting Speeds and Angle of Cut during Slant Type Taper Cutting in WEDM of Hastelloy X." *Arabian Journal for Science and Engineering* 45 (2): 641–651. doi:10.1007/s13369-019-04111-2.
- Manoj, I.V., R. Joy, S. Narendranath, and D. Nedelcu. 2019. "Investigation of Machining Parameters on Corner Accuracies for Slant Type Taper Triangle Shaped Profiles Using WEDM on Hastelloy X." *IOP Conference Series: Materials Science and Engineering* 591: 1–11. doi:10.1088/1757-899X/591/1/012022.
- Manoj, I.V., and S. Narendranath. 2019. "Variation and Artificial Neural Network Prediction of Profile Areas during Slant Type Taper Profiling of Triangle at Different Machining Parameters on Hastelloy X by Wire Electric Discharge Machining." *Proceedings of the Institution of Mechanical Engineers, Part E: Journal of Process Mechanical Engineering* 100: 1223–1242.
- Naresh, C., P.S.C. Bose, and C.S.P. Rao. 2020. "Artificial Neural Networks and Adaptive Neuro-fuzzy Models for Predicting WEDM Machining Responses of Nitinol Alloy: Comparative Study." *SN Applied Sciences* 3 (14), no. 2: 1–23.
- Naresh Chakala, P., S. Chandrabose, and C.S.P. Rao. 2019. "Optimisation of WEDM Parameters on Nitinol Alloy Using RSM and Desirability Approach." *Australian Journal of Mechanical Engineering*. doi:10.1080/14484846.2019.1681239.
- Naveed, R., N.M. Mufti, K. Ishfaq, N. Ahmed, and S. A. Khan. 2019. "Complex taper Profile Machining of WC-Co Composite Using Wire Electric Discharge Process: Analysis of Geometrical Accuracy, Cutting Rate, and Surface Quality." *The International Journal of Advanced Manufacturing Technology* 105 (1–4): 411–423. doi:10.1007/s00170-019-04150-x.
- Nayak, B.B., and S.S. Mahapatra. 2016. "Optimization of WEDM Process Parameters Using Deep Cryo-treated Inconel 718 as Work Material." *Engineering Science and Technology, an International Journal* 19 (1): 161–170. doi:10.1016/j.jestch.2015.06.009.
- Puri, A.B., and B. Bhattacharyya. 2003a. "Modelling and Analysis of the Wire-tool Vibration in Wire-cut EDM." *Journal of Materials Processing Technology* 141 (3): 295–301. doi:10.1016/S0924-0136(03)00280-2.
- Puri, A.B., and B. Bhattacharyya. 2003b. "Modelling and Analysis of the Wire-tool Vibration in Wire-cut EDM." *Journal of Materials Processing Technology* 141 (3): 295–301.
- Raj, S., Oliver Nesa, and S. Prabhu. 2017. "Modeling and Analysis of Titanium Alloy in Wire-cut EDM Using Grey Relation Coupled with Principle Component Analysis." *Australian Journal of Mechanical Engineering* 15 (3): 198–209. doi:10.1080/14484846.2016.1251077.

- Sanchez, J.A., J.L. Rodil, A. Herrero, L.N.L.D. Lacalle, and A. Lamikiz. 2007. “On the Influence of Cutting Speed Limitation on the Accuracy of wire-EDM Corner-cutting.” *Journal of Materials Processing Technology* 182 (1–3): 574–579. doi:[10.1016/j.jmatprotec.2006.09.030](https://doi.org/10.1016/j.jmatprotec.2006.09.030).
- Sarkar, S., K. Ghosh, S. Mitra, and B. Bhattacharyya. 2010. “An Integrated Approach to Optimization of WEDM Combining Single-Pass and Multipass Cutting Operation.” *Materials and Manufacturing Processes* 25 (8): 799–807. doi:[10.1080/10426910903575848](https://doi.org/10.1080/10426910903575848).
- Selvakumar, G., K.B. Jiju, S. Sarkar, and S. Mitra. 2016. “Enhancing Die Corner Accuracy through Trim Cut in WEDM.” *The International Journal of Advanced Manufacturing Technology* 83 (5–8): 791–803. doi:[10.1007/s00170-015-7606-0](https://doi.org/10.1007/s00170-015-7606-0).
- Selvakumar, G., K.G.T. Kuttalingam, and S.R. Prakash. 2018. “Investigation on Machining and Surface Characteristics of AA5083 for Cryogenic Applications by Adopting Trim Cut in WEDM.” *Journal of the Brazilian Society of Mechanical Sciences and Engineering* 40 (5): 1–8. doi:[10.1007/s40430-018-1192-7](https://doi.org/10.1007/s40430-018-1192-7).
- Somvir, S.N., G. Dixit, and S. Kumar. 2018. “Performance Evaluation of the WEDM Process of Aeronautics Super Alloy.” *Materials and Manufacturing Processes* 33 (16): 1793–1808, [4] Kumar, S., Adam Khan, M., and Muralidharan, B. 2019. “Processing of Titanium-based Human Implant Material Using Wire EDM.” *Materials and Manufacturing Processes* 34, no. 6: 695–700.
- Suganthi, X.H., U. Natarajan, S. Sathiyamurthy, and K. Chidambaran. 2013. “Prediction of Quality Responses in micro-EDM Process Using an Adaptive Neuro-fuzzy Inference System (ANFIS) Model.” *The International Journal of Advanced Manufacturing Technology* 68 (1–4): 339–347. doi:[10.1007/s00170-013-4731-5](https://doi.org/10.1007/s00170-013-4731-5).
- Vazini, A., and S.R.A. Afza. 2013. “Teimouri, R. Parametric Study along with Selection of Optimal Solutions in Dry Wirecut Machining of Cemented Tungsten Carbide (Wc-co).” *Journal of Materials Processing Technology* 15, no. 4: 644–658.
- Werner, A. 2016. “Method for Enhanced Accuracy in Machining Curvilinear Profiles on Wire-cut Electrical Discharge Machines.” *Precision Engineering* 44: 75–80. doi:[10.1016/j.precisioneng.2015.10.004](https://doi.org/10.1016/j.precisioneng.2015.10.004).
- Zhang, G., H. Li, Z. Zhang, W. Ming, N. Wang, and Y. Huang. 2016. “Vibration Modeling and Analysis of Wire during the WEDM Process.” *Journal Machining Science and Technology An International Journal* 20: 173–186.